Materials & Design 216 (2022) 110511

Contents lists available at ScienceDirect

Materials & Design

journal homepage: www.elsevier.com/locate/matdes

Particles in coronary circulation: A review on modelling for drug carrier design

Mohamadamin Forouzandehmehr [a,b], Ibrahim Ghoytasi [a], Amir Shamloo [a,*], Soudabeh Ghosi [c]

[a] School of Mechanical Engineering, Sharif University of Technology, Tehran, Iran
[b] Faculty of Medicine and Health Technology, Tampere University, Tampere, Finland
[c] Faculty of Medicine, Urmia University of Medical Sciences, Urmia, Iran

HIGHLIGHTS

- We focus on using drug carriers to target a thrombus, inflamed surfaces, and atherosclerotic plaques in coronary arteries.
- The transport, dynamics and delivery of particles as drug carriers have been discussed reviewing patient-specific studies.
- We discuss design indications for magnetic drug carriers, site-specific action of particles, and the main forces involved.
- This review brings an original perspective on the modelling for drug carrier design considering coronary local haemodynamics.

GRAPHICAL ABSTRACT

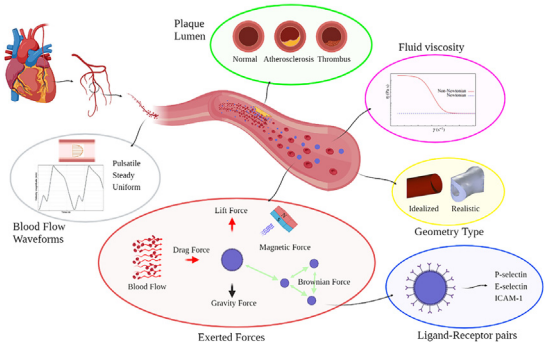

ARTICLE INFO

Article history:
Received 3 July 2021
Accepted 1 March 2022
Available online 8 March 2022

Keywords:
Drug carriers
Computer modelling
Atherosclerotic plaque
Personalised nanomedicine
Bioadhesion

ABSTRACT

Atherosclerotic plaques and thrombosis are chronic inflammatory complications and the main manifestations of cardiovascular diseases (CVD), the leading cause of death globally. Achieving non/minimal-invasive therapeutic means for these implications in the coronary network is vital and has become an interdisciplinary concern. Accordingly, smart drug delivery systems, specifically based on micro- and nanoparticles, as a promising method to offer non/minimal-invasive therapeutic mechanisms are under active research. Notably, computational models enable us to study, design, and predict treatment strategies based on smart drug delivery systems with less time and cost compared with conventional procedures in interventional cardiology. Also, the optimisation and development of computational methods and models have created a broad and practical insight into patient-specific drug design and therapeutic interventions. This review discusses the most recent works on the transport, dynamics, and delivery of particles as drug carriers to target thrombus, inflamed surfaces, and atherosclerotic plaques. Towards understanding and producing optimised particle-based cardiovascular drug delivery systems, this review conveys an original and multifaceted image on the modelling for drug carrier design.

* Corresponding author at: School of Mechanical Engineering, Sharif University of Technology, Azadi Ave., Tehran, Iran.
E-mail address: shamloo@sharif.edu (A. Shamloo).

https://doi.org/10.1016/j.matdes.2022.110511
0264-1275/

Contents

1. Introduction

Atherosclerosis in the arterial network surrounding the heart elicits several cardiac conditions called CVD. The arterial walls hardening and the reduction of the lumen cross-sectional area are two factors that define atherosclerosis. The alteration in cardiovascular haemodynamic behaviour, in various degrees, is induced by forming a thrombus which, in essence, is the result of breaking an atherosclerotic plaque. Markedly, the aggravation of such process can ultimately cause ischaemic strokes and myocardial infarctions (MI) [1]. The conventional treatments for atherosclerotic plaques and thrombosis have been updated and corrected continuously. But the invasive character of such treatments and the substantial restenosis risk demand development of new therapeutic plans [2–4]. Using micro- and nanoparticles as a means for delivery of therapeutics is a promising field in modern nanomedicine which is under active research [5–10].

According to different vascular sections, the atherosclerotic plaques previously have been categorised into five major anatomical categories, using clinical data from 13,827 patients, by Debakey and his colleagues [11]. These anatomical regions include main, visceral, and terminal branches of abdominal aorta, the major arteries dividing from aortic arch, the coronary network, and the two of the mentioned groups combined. Also, clinical autopsy studies indicate that the development of atherosclerotic plaques are more prone at the proximal segments of left and right main coronary arteries [11]. Finally, it is nevertheless noteworthy that the haemodynamic factors have been hypothesised, for many years, as major contributions to the process of vascular remodelling [11].

The inflammation is considered the initiation phase of developing atherosclerotic plaques and vascular diseases in cardiac network of vessels. Correspondingly, in this specific field, the controlled release of drug carriers of different sizes and shapes along with their near wall movement (margination) have been heavily studied [12–17]. These investigations cover targeting the inflammatory or tumour-associated antigens on surfaces of the cells and also develop our understanding of the optimisation of targeted drug delivery designs. In that context, the interplay of hydrodynamic forces, the particle transport, and effectual interactions with targeted cell surfaces are key components of every smart vascular drug delivery system which employ micro and nano particles. Importantly,several factors make the *in vivo* analysis and measurement of targeted drug delivery system indices very challenging ,namely, the nanoscale size of the carriers, the complex vascular biochemical environment, the dynamics and nonlinearity of the delivery process, the metabolism and clearance of the drug, and extravasation among different barriers [18]. However, non-invasive, lucrative, and rather accurate means to attain this information can be within reach by using verified mathematical tools. These mathematical tools here translate to well-established computational particulate fluid dynamic which can simulate transport of diluted species. In fact, computer-based modelling assists us to understand and explore the graded complexity of pathophysiological phenomena across several scales. Also, particularly in nanomedicine, this approach plays an essential role in supporting the progress and improvement of patient-specific therapeutic methods [19–22].

In a nutshell, this review discusses the significant works (Table S1 in Supplementary Materials) on the use of particles as drug carriers and/or diagnostic agents to target a thrombus, inflamed endothelium, and atherosclerotic plaques with a focus on the coronary arterial network. We also deliberate on flow and geometrical characteristics involved in the transport, mechanics, adhesion, and delivery of particles (Fig. 1) to convey an original and multifaceted image on the modelling for micro- and nano drug carrier design.

2. Patient-specific multi-scale modelling: assumptions & methods

Implementing a multi-scale mathematical model to study bioadhesion, transport, and interaction of micro- and nanoparticles with the targeted areas in coronary haemodynamics is of great importance. Here, the integrated continuum particle-based approaches such as computational fluid-particle dynamics is a good example. In different flow scales, such models have been used and proved to be a successful method to research the pathophysiology of arterial networks [23–30]. Of note, reviewing such models as well as implementing them is challenging and needs sufficient and careful consideration regarding the pathophysiology of the targeted area of study and computational haemodynamics. For instance, Epshtein and Korin [31] have highlighted that the reported high particle deposition at the stenotic lumen compared to the low deposition at the post-stenotic area of the plaque in this

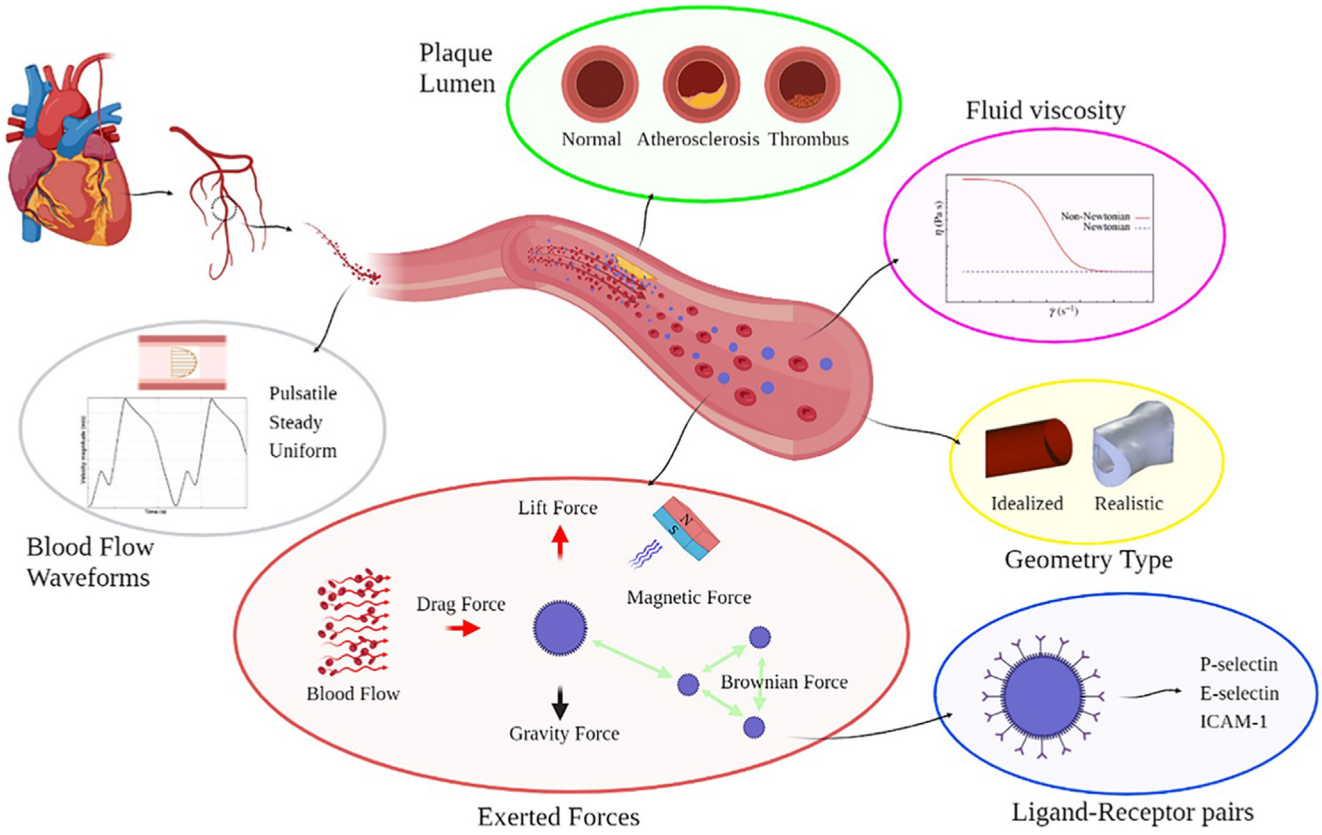

Fig. 1. Particles in coronary circulation and modelling for drug carrier design (created in biorender.com).

in silico model [32] is not consistent with the experimental results in [33]. Importantly, we believe a number of facts in the cited experiment challenge this analogy and the subsequent conclusion. Namely:

a) The experiment [33] was done at Newtonian and constant flow rate and static shear rate at each scenario. Whereas the computational model [32] simulates the particle delivery at non-Newtonian blood with dynamic flow rate and shear rate in every simulation.
b) The experiment assumes physiological and pathological wall shear stresses (WSS) equal to 2 and 60 Pa, respectively. However, in consistent with experimentally reported WSS in the left anterior descending artery (LAD) [34], the computational model simulates the pathological WSS at the plaque lumen equal to 2.5 Pa.
c) Even in the experiment, the boosted vWF A1- nanoparticles deposition at post-stenotic region at 60% stenosis mode in collagen-vWF coated surface, does not occur at the 75% stenosis. Nor does it happen at 60% stenosis scenario where the surface was coated with collagen alone.
d) The experiment has been done considering 60 and 75% of an idealistic concentric occlusion. Whereas the computational model simulates 56.3% patient-specific realistic occlusion with luminal unevenness. Further, the pathological and physiological arterial bed in the experiment have been modelled uniform. Yet, in the computational model the arterial geometry captures luminal unevenness.
e) Finally, in a high-haematocrit (65%) non-Newtonian blood flow where the exerted WSS in the plaque domain is higher compared to normal (45%) haematocrit, the computational model has simulated significant post-stenotic particle deposition [35] in accord with the trend supported by the experimentalists [31].

Another important factor in the development and use of computational methods is the investigational domain. Based on the scale of investigating domain, different mathematical methods can be employed to study the flow of blood. To be specific, in arteries with diameters larger than 500 μm, e.g. LAD in coronary network [36], the existing high flow rate allows us to model the fluid characteristics and fate accurately by employing continuum methods [37]. As arterial diameters become smaller than 500 μm, the nature of blood flow turns out to be more non-Newtonian, nonetheless it can be modelled by continuum assumptions [37].

But as previously studied [15], for vessels less than 100 μm in diameter, Red Blood Cells (RBC) must be explicitly modelled [38]. Despite this, various studies have been conducted to evaluate the efficiency of targeted drug delivery systems with different approaches, which have not explicitly modelled RBCs [23–25]. Those studies have shown that, fluid variable viscosity and the effect of lumen unevenness have caused heterogenous distribution of particles in the cross section of the vessel. Apart from these factors, there are two other important characteristics that can influence the particle distribution path; 1) The significant instant variations of fluid velocity magnitude in the circulation in the LAD artery and its effects at the site of occlusion. 2) The lumen walls movement captured in the fluid-solid interaction (FSI) method and the compliant vessel wall assumption. It has also been shown that, despite the lack of explicit modelling of RBCs, if non-spherical particles have adequate inertia, they drift laterally toward the vessel wall, even at a linear laminar flow with a constant shear rate [26,39]. Indeed, the important factors such as rapid variation and nonlinearity in flow rate, interparticle interactions as well as asymmetry of the geometry of the desired system cause a unique heterogeneous distribution across the cross section of the lumen for spheres and non-spherical particles.

As a well-established fact, at cell and organ levels, the safety of therapeutic and clinical interventions is highly influenced by the

patient's specific characteristics [40,41]. Nowadays, we know that the clinical trials outcomes do not necessarily apply to patients in variety of conditions. More interestingly, this remains true even for patients who participated directly in the trial [42,43]. Particularly, in coronary artery diseases, the geometric features of the arterial structure and atherosclerotic plaque vary from person to person and depends on the patient's pathological conditions. In this case, the age, genetic background, and anatomical characteristics of each patient can feature large in how drugs are distributed, metabolised, consumed, and broken down in the body, and even their biochemical effects on target cells. It is noteworthy that multi-scale computational modelling in nanomedicine can significantly contribute to developing and improving personal treatment approaches [19,44–46]. Personalised computational medicine have recently emerged as a powerful framework in disease treatment. In this context, interdisciplinary studies on cardiovascular diseases have addressed critical pharmaceutical, pathophysiological, and haemodynamic indices along with calibration of high-performance personalised computational models [47–49].

The FSI method mainly has been used to realistically describe the fluid flow and the solid wall displacements considering the involved interactions. Hossain et al. [50] studied the process of nanoparticle transport and uptake in a drug delivery simulation of a diseased superficial femoral artery (SFA). They provided new insights into the progression of atherosclerosis. Although, in this model [50], they used MRI-based data of fluid flow as a more realistic description of blood flow and assumed the arterial wall as a non-compliant solid. Nonetheless, this model could not observe the effects of wall displacements on particle adsorption and particle–wall interactions.

In addition, it has been found that the modelling of a non-Newtonian blood can lead to a better results consistency with experimental WSS data, compared with a Newtonian blood flow assumption [37,51–53] as blood is inherently a non-Newtonian fluid and this becomes even more significant when the haemodynamic nature of LAD with highly rapid WSS oscillations is of concern.

3. Indications for drug carrier design & simulation

High bioadhesion probability, the capability to move near the vessel walls (marginate), and the proper density of particles at the drug-cell interaction sites, have made the design of drug carriers challenging. Apart from these factors, the distribution of micro- and nanocarriers within the cross-section of the vessel, especially at the site of the lumen plaque, is directly involved in drug delivery success [15]. This factor depends on the biological aspects of the human body and the structure of the particles. Explicitly, body features including blood flow characteristics, namely, haematocrit and vessel size can be influential. In addition, the structural properties of particles such as the size and shape of drug carriers have significant influence on the distribution of micro- and nanoparticles within the arterial and needle cross-section [36,54].

Considering blood and drug-carrying particles floating in it as a dispersed flow can be a useful and correct assumption. This means that the volume fraction of blood, the continuous phase, is much greater than the volume fraction of particles which is less than 1%. In other words, the particles occupy a limited space inside the blood and do not displace it. Consistently, this assumption is maintained for different doses of fibrinolytic drugs administered in the coronary circulation [55,56].

Kent et al. [42] studied the therapeutic effects of drug carriers in clinical trials. In this study, they investigated the effects of particle size (from nano to micro size) and geometry (from complete spheres to nearly rod-shaped particles). In this work, they have considered the particle size range calculatedly different from the standard recommended diameters for nano drug carriers (10–200 nm [57]) since the refinement of the particles larger than 200 nm by the liver and the renal clearance of those smaller than 10 nm are not critical when delivering thrombolytics is concerned. Another factor to consider here is the temporal features of the treatments based on thrombolytics. In fact, in MI, thrombolytics are administered usually within the hour of onset of symptoms (angina pectoris). [58–60]. Secondly, due to the internal haemorrhage risk, it is important that these agents remain in the circulatory system for a short amount of time. Also, their usage is innately different from the pharmaceuticals that developed to have a longer half-life in the body. Furthermore, to reduce the risk of internal bleeding due to the dissolution of healthy clots in the body, the clot-targeting carriers are specially developed with high affinity to the disease site as well as high site-specific action. This allows reaching an optimal effect with minimum administered drug dose, maintaining a minimal systemic circulation of thrombolytics.

Given the above, the migration of drug carriers toward thrombus and the targeted tendency of micro- and nanocarriers to the desired sites are among the important features that should be considered in the design of this type of drug. Of note, considering shear-activated drug carriers and their remarkable efficacy in thrombolytic therapies [61], a variety of drug carriers have been designed. Previously [32,36], particle sizes and shapes have been selected to include a wide range of drug carriers, ranging from silicon carriers and elongated liposomes to micron-sized shear-activated aggregates.

Notably, in case of optimal delivery of drug carriers featuring ligand-receptor mechanism, an interesting index of evaluation is Particle Residence Time (PRT). To clarify, in the LAD artery and its branches, the more slowly particles move, the longer they locate near diseased endothelial cells, thus the higher becomes the chance of adhesion (delivery). This index of assessment has been studied in a patient-specific research focusing on the effect of particles material and population on the final delivery to an LAD atherosclerotic plaque [62]. For 800 and 1000 nm particles, as the number of injected particle increases, the surface density of attached particles (SDA) on the plaque increased meaningfully. However, dissimilar trends of SDA were observed when constant number of particles were injected in different sizes. In the next phase, the delivery and distribution of nanoparticles with metal cores such as SiO_2 (2650), Fe_3O_4 (5170), NiO_2 (6670), Silver (10490), and Gold (19300) were simulated with respect to their densities (numbers in parentheses in Kg/m^3). In the patient-specific geometry of the studied LAD, the highest SDA was observed for Fe_3O_4 and Silver particles when constant number of particles was injected. The authors also showed that the margination of those particles is significantly higher compared with the rest using Poincare maps. Of note, the final SDA was significantly more influenced by the ligand-receptor pairs affinity, the geometrical indices, and the biophysical features involved in the adhesion rather than different densities of particles. Ultimately, the PRT and the SDA in the studied domain were decreased for all particles after the inclusion of Saffman lift force [62].

Importantly, PRT can also demonstrate the impact of coronary flow, specifically, on valves haemodynamics in transcatheter heart valve leaflet (THV) thrombosis in the neo-sinus [63]. This condition is associated with a reduced leaflet motion which poses risks of embolism and thus holds serious clinical concern. Madukauwa-David et al., in an experimental study using high speed particle image velocimetry (PIV), showed that, unlike in the intra-annular valve, the blood flow motionlessness in the supra-annular THV neo-sinus and, apparently, thrombosis risk in the region are reduced due to the coronary flow [63].

4. Margination and thrombus

In physiology, the lateral movement (drift) of leukocytes toward the endothelial walls is commonly described by a well-known term called Margination [64,65]. Accordingly, marginating particles are particles that move specially near the luminal surface. And the meaning of margination dynamics is the lateral movement of particles from inside the bloodstream to the vessel walls [64]. A variety of biochemical processes are performed to modulate the drift of leukocytes towards the vessel wall and the tendency of RBCs to move along the central line of blood flow in the vessel. At the same time, the movement of inorganic drug-carrying particles generally depends on their shape and morphology [65]. It should also be noted that the margination of drug-carrying particles is profoundly affected by gravitational forces and other similar external fields. But the physiological margination in our bodies operates independently of these types of fields [65].

The margination of suspended particles and cells, including White Blood Cells (WBCc) [66,67], platelets [68,69], and rigid microparticles [70,71] has been observed experimentally within the microcirculation, arterioles and venules. How the geometrical characteristics of the particles affect the efficiency of drug delivery depends on many conditions and parameters. Particles with a characteristic diameter greater than 4 μm are likely to get stuck in the smallest capillaries in the body [72]. In addition, it has recently been shown by microfluidic experiments that the adhesion density of 2 μm particles is significantly higher than that of 200 nm and 500 nm particles [13]. Experimental [14,73] and theoretical [74,75] studies of the behaviour of particles with different shapes have shown that, in the same volume, the adhesion ability of oblate ellipsoidal particles is higher than spherical particles. Recently, an *in vivo* study has been performed to investigate the application of drug delivery in atherosclerosis. In this study, drug-carrying spherical microparticles were used. Based on the results, for better delivery and adhesion of the drugs to the arterial occlusion sites, they emphasised that the size and shape of the drug-carrying particles should be strongly considered in the design of drug-carrier based systems [76]. In coronary arteries, a better understanding of the optimal micro- and nano drug carriers delivery, the bioadhesion strength, and the influence of particle size and shape, can be achieved by quantitative studies in a realistic model of blood flow.

Glagov et al. reported that lumen occlusion of 40% is a critical threshold for the manifestation of coronary heart disease (CHD) symptoms [77]. In this condition, a restrained blood flow speed leads to an altered haemodynamics and decrease in the volumetric blood flow. At this stage, when the patient feels angina, thrombolytic drugs are administered within the first hour of the onset of symptoms [58–60]. Therefore, unlike cancer studies, due to the nature of the disease and the therapeutic perspective, in the study and modelling of thrombolytic therapies, especially through micro and nanoparticles as targeted drug carriers, the movement of drug carriers towards the walls in areas of the lumen with high potential of thrombus existence (PTE) is expected. Accordingly, Forouzandehmehr and Shamloo tested and suggested this criterion of particle margination for the design of thrombus-oriented drug carriers [36].

5. Convection-diffusion mode and diseased endothelium

The study of diseased endothelial cells (ECs), the inflammatory process, and its consequences are among the main concerns of modern nanomedicine, specifically, targeted delivery of site-specific action therapeutics. This type of dysfunction, which is prone to myocardial infarction, is profoundly affected by the increased density of surface adhesive molecules such as intracellular adhesion molecule-1 (ICAM-1), E-selectin, and P-selectin in the disease area [78]. Notably, the location of the accumulation of these molecules can be used as targets for diagnosis and therapies with the micro and nano drug carriers [79]. The application of non-invasive methods in the recognising and anatomically locating the EC dysfunctions, significantly increases the ability to diagnose and treatment of inflammation in the cardiovascular system and atherosclerotic plaques. Several studies have focused on targeting components such as antibodies, natural receptors, and minimal sequences of binding peptides. These studies have confirmed the potential of non-invasive methods in the diagnosis and treatment of atherosclerotic plaques, angiogenesis, as well as myocardial ischaemic memory and organ transplant rejection [79–83].

It has been physiologically proven that in all atherosclerosis phases from the beginning to the progression and finally until the onset of thrombus formation the local inflammation is present [84]. As a result, one of the most promising ways to diagnose and treat this type of disease is to target local inflammation [84]. Correspondingly, local inflammation has been proved to be a chief cause of composition and formation of atherosclerotic plaques [85].

The site-specific delivery of particles covered with special proteins to a LAD atherosclerotic plaque has been also simulated [32]. For different particle sizes and covering ligands the final SDAs were computed. In this patient-specific study, authors showed that the affinity constant and the specific diffusivity of ligand-receptor bonds, in the dynamic ligand-receptor adhesion, directly affect the final amount and homogeneous density of adsorbed particles on the surface. The modelling also shows that depending on the type of ligand-receptor bonds, the results obtained do not depend significantly on the different sizes of drug-carrying particles. In addition, for the studied LAD artery, an optimal state of the ligand-specific dual-targeting arrangement of 800 nm particles on the plaque surface is presented. The proposed ligand arrangement resulted in a homogeneous distribution and a significant SDA.

Correspondingly, in another patient-specific study, adhesion of micro and nanoparticles on a LAD atherosclerotic plaque has been investigated in high haematocrit (Hct) blood flow [35]. To study delivery of particles ranging from 200 to 3200 nm, a LAD arterial geometry capturing the luminal unevenness was made and meshed by the finite element method. The cell adhesion model proposed in [75] was adopted to model the binding kinetics of particles decorated with P-selectins. In compare with the particles travelled in normal blood Hct (45%), distribution of adhered particles on the targeted cells was significantly more homogenous in high blood Hct. Of note, the homogeneity index used for the evaluation was defined based on the concentration gradients in Cartesian directions at the last time step of the simulations [35]. From 800 nm particles onwards, the increase in the SDA over the targeted surfaces was significantly more influenced by increase in particle diameter in normal level of blood Hct. Remarkably, dissimilar to the results of normal Hct, a momentous distribution of deposited particles was observed in the post-stenotic area of the atherosclerotic plaque in the high blood Hct (65%).

6. Magnetic drug carriers

The process of releasing the drug from the carrier particles can be triggered by environmental factors inside and outside the body such as pH, temperature or magnetic field [23]. The ability of magnetic fields to penetrate the human body to remotely detect and control the magnetic materials in it, have been studied in medicine for centuries [86]. Magnetic Drug Targeting (MDT) is one of the best ways to overcome the problems of efficiently transporting and delivering drugs to any desired location of the body to treat

diseases; the goal that scientists of nanomedicine have been pursuing from the beginning [87–90].

Magnetic nanoparticles as a therapeutic tool for targeted drug delivery [91] have been extensively studied and evaluated, mainly with the aim of enhancing the ligand-receptor bindings with high affinity [92,93]. Hitherto, many studies have been conducted regarding the applications and effects of magnetic fields on arterial drug delivery and atherosclerotic plaques [28,94–97]. It should be noted that, the use of disease biomarkers combined with the magnetic impact is among promising capabilities is considered an outstanding capability in targeted drug delivery. These capabilities make magnetic nanoparticles a viable option for remotely directing therapeutic agents exactly to the site of disease, and also make it possible to use lower doses of drugs. At the same time, it reduces the adverse side effects of cytotoxic drugs on the healthy tissues around the diseased site. Also, the use of colloidal iron oxide particles as targeted drug carriers in early clinical trials has been somewhat successful and faced satisfactory toleration from the patients [98].

Numerical evaluation of the distribution of targeted drug carriers in the vascular system of the brain was performed by Kenjereš and Righolt [28]. This study demonstrates the superiority of the MDT method in the non-invasive treatment for brain tumors. Furthermore, in MDT studies on bifurcations, Larimi et al. showed that the magnetic field can cause magnetic particles to accumulate at the targeted site, but the higher the Reynolds number in the bloodstream, the lower the efficiency of the method [96]. In addition, they found that using the MDT method increased the number of settled nanoparticles in the carotid artery [95]. In another study, they showed that under the influence of various factors, using the MDT method in bifurcations is more effective for a diabetic patient than a healthy person. Apart from that, they reported that due to the biophysical nature of blood, the magnetic field does not affect it [99]. Control and guidance of drug-carrying particles by magnetic field in realistic and Y-shaped models of brain vessels was studied in [97]. They developed a field-based method for distancing particles from walls and transporting them to the desired location, which increases separation efficiency. Krafkick et al. computationally investigated the behaviour of nanoparticles in the lung alveolus [98]. In this research, the effects of magnetic, gravitational, and drag forces on nanoparticles have been evaluated. Considering the low viscosity of the blood flow in the lungs, they reproted that the magnetic force overcomes drag and gravitational forces and has a greater effect on the behaviour of nanoparticles. The problem of drug delivery with drug-carrying particles affected by the magnetic field was also studied by Boghi et al [100]. This study showed that when using the MDT method to achieve optimal therapeutic conditions, the distance of the magnetic field source from the desired location in the coeliac trunk should be considered [100]. Treatment of diseases in a realistic geometry of the lower [98], central, and upper [101] respiratory systems of the human body has been evaluated through targeted delivery of magnetic aerosols drug carriers. Studies show that the two main factors that increase the particles adhesion to the desired surface are the magnitude of the applied magnetic field and the size of the particles.

Although magnetic fields have so far been utilised to effectively treat human diseases, the magnetic targeting with external magnets have mostly been used for targets located at superficial tissues [102]. Nonetheless, recently, noteworthy efforts have been made to provide reliable methods for overcoming the challenges of deep-focusing in targeted sites, resulting from homogeneous magnetic fields [87,88]. In the meantime, Nacev et al. proposed an experimental procedure to produce deep-focusing therapy based on a magnetic field controlled by externally placed magnets [88].

As an experimental combined therapy, a deep-penetrating delivery approach has been tested for a stented coronary artery using ultrasound stimulation and magnetic guidance to overcome in-stent restenosis (ISR) [103]. In this study, the PLGA nanoparticles loaded with antiproliferative drug is surrounded by shells which are coated microbubbles with magnetic nanoparticles. Also, a focused ultrasound with low intensity was applied to stimulate steady oscillations of microbubble. This, as a trigger, leads to PLGA-PTX release when being targeted to the stent influenced by the magnetic field. Interestingly, the generated microstreaming improved the smooth muscle cells (SMCs) internalization of released PLGA-PTX, thus decreasing the clearance due to the blood flow. Importantly, the drug accumulation at the stented region was improved by 10 folds due to the magnetic targeting. Furthermore, cellular uptake, drug penetration, and the drug retention time were enhanced due to the applied low intensity focused ultrasound [103].

On the computational side, specifically guided magnetic fields can considerably influence the particles to marginate in a non-Newtonian solved blood flow and subsequently elevate the binding chance of particles to the targeted receptors [104]. In this study, the effect of inclusion of Brownian forces were reported significant (4 folds increase) on the delivery of 400 nm particles. On the other hand, the effect of accounting for the gravitational force on the SDA of 1000 nm particles was reported insignificant. Finally, the magnetic field most significantly improved the SDA of 600 nm particles and adversely affected the SDA of 800 and 1000 nm particles.

Moreover, the application of continuous, rapidly shaped magnetic pulses to ferromagnetic rods creates an internal stable quasi-static magnetic field. The generated magnetic field allows the ferromagnetic rods to be concentrated in the desired location by external magnets [88]. Likewise in this regard, the investigations on drug-carrying magnetic particles under magnetic fields controlled by external magnets are outstandingly increasing in various parts of the human body, including carotid arteries and intracranial vasculature [89,90,95].

7. Site-specific action and adhesive dynamics simulations

There are number of models for calculation of the general adhesion strength [105–108]. The bioadhesion model articulated by Decuzzi and Ferrari [75], is one of the most famous, in which the general adhesion strength, P, directly correlates with the higher chance of successful bonds of particles to the designated receptors. For particles of spherical shape, it yields:

$$P = \pi r_0^2 exp\left[-\frac{\lambda}{K_B T}\left[6(a+\delta_{eq})F^S + 8\frac{a^2}{r_0}T^S\right] \times \frac{a}{r_0^2}\frac{\mu S}{m_r}\right]\left(m_r m_l K_a^0\right) \quad (1)$$

$$r_0^2 = a^2\left[1 - \left(1 - \frac{h_0 - \delta_{eq}}{a}\right)^2\right] \quad (2)$$

where the F^S and T^S are coefficients that hinge upon the aspect ratio of particles ($\gamma = a/b$), for spheres ($\gamma = 1$) according to Goldman et al. [109] $F^S \cong 1.668$ and $T^S \cong 0.944$. Here, the probability of forming at least one ligand–receptor bond is defined as the probability of adhesion P. In the Eqs (1) and (2), a represents the spherical particle radius, the equilibrium parting distance between the vascular substrate and the particle is denoted by δ_{eq}, h_0 represents the maximum distance a particle can have from the lumen at which a specific bond forms, K_a^0 represents the association factor for ligand–receptor bonds bearing no load, r_0 represents the circular section radius of the spherical particle placed at a separation distance denoted by h_0 from the substrate, λ represents the reactive compliance, $K_B T$ is the thermal energy of Boltzmann, and μS denotes the wall shear stress.

Outstandingly, the strength of adhesion for spherical particles increases by the increase in the surface density of the receptors m_r, the ligands m_l, and the affinity constant K_a^0 [110–113]. One of the prominent features of inflammation and atherosclerotic plaque formation is the difference in the expression level of specific receptor molecules in the disease area. Specifically in such pathologies, the most prevalent receptors involved in transient and firm adhesion of circulating immune cells to the inflamed endothelium are E-selectins, P-selectins, and intracellular adhesion molecule-1 (ICAM-1) [114]. Inspired by this fact, the antibodies able to react to molecular markers of the disease molecular markers can be P-selectin aptamer (PSA), Sialyl Lewis^x (sLe^x), and ICAM-1 antibody (abICAM). Given, the targeting drug carriers covered with such ligands can be designed as a promising step towards site-specific delivery/diagnostic method [32,78]. Hence, in the simulations, m_r must be set according to the quantity of these expressions over the inflamed endothelium.

In 2010, Maul et al. [78] have used a range of values for surface density of some endothelial receptors, namely, E-Selectin, P-Selectin, and ICAM-1 which was 3.5 to 2.7 $\times$ 10^{15} m^{-2} according to a study done by Weller et al. [115]. In fact, m_r becomes significantly higher over the inflamed or activated endothelial cells. Consequently, Shamloo and Forouzandehmehr [32] used the highest value of the range (2.7 $\times$ 10^{15} m^{-2}) as the value representing an abnormally high receptor surface density on an inflamed lumen. Correspondingly, the selected value for m_r is analogous to E-Selectin surface density on the inflamed ECs (3.7 $\times$ 10^{14} m^{-2}) according to [116]. In a recent study [32], the surface of an atherosclerotic plaque, as a uniformly inflamed surface, has been assumed to have a pathologically high surface density of receptors expression denoting inflamed or activated ECs; consistent with previous studies on different kinds of inflammatory luminal diseases [78,116].

Finally, in protein targeting, the particle adhesion to the inflammatory markers and optimising the ultrasound contrast agents are heavily influenced by the affinity components ($K_a^0 = \frac{k_f^0}{k_r^0}$, and forward and backward intrinsic kinetic rates) [32,78]. Thus, the values for K_a^0 and m_r can properly be selected and used depending upon the atherosclerotic plaque surface chemistry and the specific kinetics of the ligand-receptor pairs.

Specific diffusivity and reactive compliances of ligand-receptor bonds have also been the parameters which were considered in simulations and experiments [32,78]. The effects of which on the final distribution of adhered mono and dual-targeting drug carriers on a LAD athersclortic plaque have been stduied recently [32]. Notably, specific diffusivity of bonds in dual-targeting carriers can have a signficant influence on the final homogenity of distribution of adsorbed particles on the targeted location. In a patient-specific study, Shamloo and Forouzandehmehr introduced 800 nm spherical carriers with 4.9% PSA and 95.1% sLex covering ligands as the optimal ligand arrangement that results in a significant SDA and meaningfuly imporved particle deposition homogeneity over the plaque [32]. Fig. 2 illustrates different computational approaches taken on studding a patient-specific LAD coronary artery.

8. Forces exerting on particles in motion

Lagrangian Particle Tracking (LPT) is a capable and applicable tool in studying the fate of released particles in simulated blood flow. In the LPT simulations, the forces applied on particles are separated into two collections, the external forces and those due to interparticle interactions. To calculate the formers researchers widely use the finite element methods. Explicitly, for each direction of the position vector, there is a second order ordinary differential equation (ODE) needed to solve for each particle. Moreover, at the present position of the particle, for each time step, the external forces are calculated and included. Lastly, the interparticle forces are added to the total calculated force. Consequently, the position of particle will be updated. This process repeats until the simulation reaches its designated end time. The nanoparticles trajectories and velocities can be calculated by integrating:

$$\frac{d}{dt}(m_p\mathbf{v}) = \mathbf{F}_D + \mathbf{F}_L + \mathbf{F}_B + \mathbf{F}_g + \mathbf{F}_{mp} \quad (3)$$

where m_p denotes the mass of particles, $\mathbf{v}$ is the vector of velocity of each particle, $\mathbf{F}_D$ represents the drag force, $\mathbf{F}_L$ is the Lift force, $\mathbf{F}_B$ is

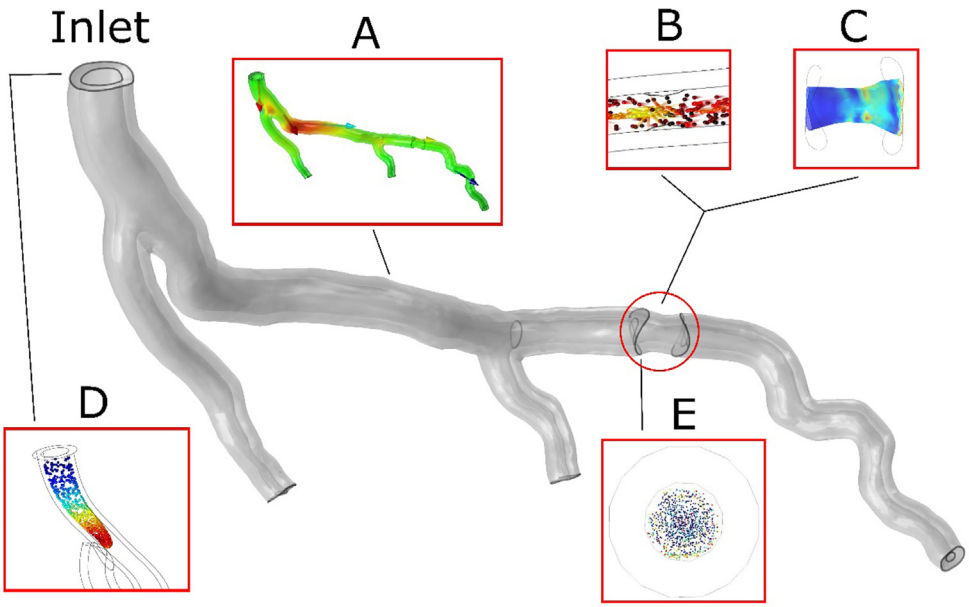

Fig. 2. Computational modelling of a pathological LAD, (A) a displacement map of the arterial wall in FSI simulations, (B) particle-particle interactions and density of drug carrier particles in the plaque domain, (C) a deposition map of adhered particles on the plaque lumen, (D) injection of particles into the pulsatile fluid flow, and (E) Poincare map of dense presence of drug-carrying particles in the cross-sectionof plaque domain.

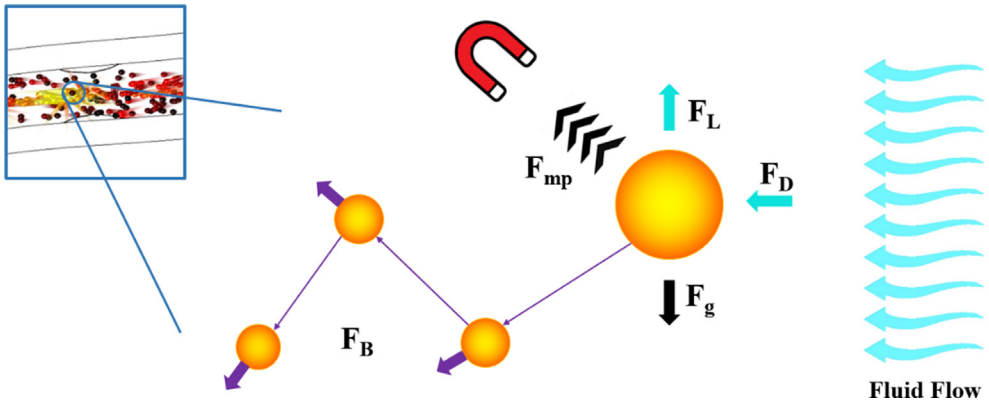

Fig. 3. Several types of forces (F_D; Drag force, F_L; Lift force, F_B; Brownian force, F_g; Gravitational force, F_{mp}; Magnetophoretic force) applying on the particles in the fluid flow.

Table 1
The values for the drag coefficients in a range of Reynolds number (Re_r) [118].

Range	Relationship
$Re_r \leq 0.01$	$C_D = 4.5 + 24Re_r^{-1}$
$0.01 < Re_r \leq 20$	$C_D = 24Re_r^{-1} + 3.156Re_r^{-0.18-0.05\log Re_r}$
$20 < Re_r \leq 260$	$C_D = 24Re_r^{-1} + 4.644Re_r^{-0.3695}$
$260 < Re_r \leq 1500$	$\log C_D = 1.6435 - 1.1242\log Re_r + 0.1558(\log Re_r)^2$

the Brownian force,$\mathbf{F}_g$ represents the Gravitational force and $\mathbf{F}_{mp}$ denotes the Magnetophoretic force. In the fluid flow, the forces that affect the path of the drug-carrying particles are shown in Fig. 3. These forces are briefly described below.

8.1. Drag force

The drag force applying on each particle in the flow is given as [117]:

$$\mathbf{F}_D = (\frac{1}{\tau_p})m_p(\mathbf{u} - \mathbf{v}) \tag{4}$$

where τ_p is the relaxation time of particles, defined as:

$$\tau_p = \frac{4\rho_p d_p^2}{3\eta_{app} C_D Re_r} \tag{5}$$

where ρ_p is the particle density, d_p is the diameter of particles, C_D denotes the drag coefficient, η_{app}represents the apparent dynamic viscosity of blood, and Re_r represents the relative Reynolds number of particles:

$$Re_r = \frac{\rho\|\mathbf{u} - \mathbf{v}\|d_p}{\eta_{app}} \tag{6}$$

where ρ represents the fluid density encompassing the particles. The drag coefficient calculation can be based on standard drag correlations. These correlations depend on the relative Reynolds number as reported in [118], shown in Table 1.

Markedly, to include the influence of shape of particles in the targeted drug delivery simulations researchers have used drag coefficients with empirical correlations for particle sphericity [36].

8.2. Lift force

When particles are transported in a fluid with an inhomogeneous velocity field, lift forces are applicable. The wall induced and Saffman lift forces are at play when particles move in a creeping flow. In fact, the particles positioned far from walls are influenced by Saffman lift force. The Saffman lift force [119], is calculated by Eq. (7) and the parameter L_v is defined by Eq. (8)

$$\mathbf{F}_L = -81.2r_p^2 L_v\sqrt{\mu\rho\frac{|\mathbf{u} - \mathbf{v}|}{|L_v|}} \tag{7}$$

$$L_v = (\mathbf{u} - \mathbf{v}) \times [\nabla \times (\mathbf{u} - \mathbf{v})] \tag{8}$$

where r_p denotes the particle radius, μ represents the fluid viscosity, v is the velocity of particles and u denotes the fluid velocity. Saffman lift force becomes zero when particles attain an equilibrium with the neighbouring fluid velocity. Notably, the inclusion of lift forces in a patient-specific study focusing on population of particles and their delivery to an atherosclerotic plaque, resulted in significantly lower SDAs and PRT compared with the simulations without considering lift forces [62].

8.3. Brownian force

In microscale, in comparison to the drag force, the Brownian forces responsible for the Brownian movement of particles can be neglected in the analyses [120]. But for nanoscale particles, the Brownian force can be more dramatic than the tensile force. Also, near the walls of the vessels, the Brownian force can be the dominant force for the mobility and displacement of the nanoparticles. Notably, there is an approved interval for the diffusion coefficient order i.e. between $10^{-14}to6 \times 10^{-10}$ (m^2/s) [121,122]. The Brownian Force, as a force with random nature, applies on each particle and it is represented by a Gaussian noise process at each time step [123,124]:

$$\mathbf{F}_B = \zeta\sqrt{\frac{6\pi k_B \eta_{app} T d_p}{\Delta t}} \tag{9}$$

where k_B is Boltzmann's constant, T represents the fluid temperature, Δt represents the magnitude of time step which solver takes, and ζ represents a random vector with a unit standard variation and a mean of zero which is normally distributed. To simulate the randomness, for each Brownian force component, a different value of ζ is made at each time step for each particle.

8.4. Gravitational force

The gravitational force applying on each particle travelling in the fluid can be calculated by the following equation [125]:

$$\mathbf{F}_g = m_p\mathbf{g}\frac{(\rho_p - \rho)}{\rho_p} \tag{10}$$

where, $\mathbf{g}$ represents the acceleration caused by gravity.

Selecting a proper direction for the gravitational force on the particles depends on the geometry of the problem and is based on CT scan images of the LAD artery. Depending upon the patient's configuration while implementing the magnetic field, the direction of $\mathbf{F}_g$ can be selected. For instance, in [104], this direction has been chosen to be along the **y-**axis; considering that the magnetic force would be applied on the patient when they are located in flat position.

8.5. Magnetophoretic force

Magnetic forces can be applied to the particles due to the magnetic permeability difference between the background fluid and the particles. These magnetic forces are included in the simulations in this way and they are responsible for movement of permeable particles towards the regions with a stronger magnetic field. Targeted delivery methods based on charge neutral particles can employ magnetophoretic force as long as there is a difference in the relative permeability between the background fluid and the particles. The magnetophoretic force is defined as [126]:

$$\mathbf{F}_{\mathrm{mp}} = \frac{1}{4}\pi d_p^3 \mu_0 \mu_r K \nabla \mathbf{H}^2 \tag{11}$$

where $\mathbf{H}$ is the magnetic field intensity, and K is given as

$$K = \frac{\mu_{r,p} - \mu_r}{\mu_{r,p} + 2\mu_r} \tag{12}$$

$\mu_{r,p}$ denotes the magnetic permeability of particles which is dimensionless [127].

9. Solvers and algorithms

Solving governing partial differential equations usually in combination with a finite element code or software are usually used to simulate continuum-particulate systems. The FSI simulations can be performed adopting a coupled solver that uses a direct version of MUMPS algorithm [128], a BDF time-stepping technique [129,130] and a tolerance-based termination approach. Also, a solver featuring a backward Euler with consistent initialisation incorporating the generalized alpha time-stepping technique has been used in studying particle transport simulations [131,132].

10. Conclusion

In our previous studies, different modeling techniques have been implemented for studying biological phenomena [133–136]. In this review paper, the modeling techniques for drug carrier design were discussed focusing on coronary circulation. Despite recent clinical breakthroughs, cardiovascular diseases (CVD) remain the leading cause of death and disability worldwide. Atherosclerosis, an inflammatory disease of the vascular wall, is the most common form of CVD and a major cause of ischaemic heart problem. Targeted delivery of therapeutics based on micro- and nanoparticles is a capable tactic for devising new policies in treating atherosclerotic plaques and thrombosis. In this review, the key works aimed at modelling the transport, dynamics, and delivery of particles in the coronary blood flow were discussed. We glanced at the most recent works dedicated to using particles as drug carriers to target a thrombus, inflamed surfaces, and atherosclerotic plaques. Considering manufacturing optimised and efficient drug delivery systems, the key multi-scale comprehensive modelling investigations addressing the modern approaches in the treatment of coronary network diseases were discussed in this article.

Declaration of Competing Interest

The authors declare that they have no known competing financial interests or personal relationships that could have appeared to influence the work reported in this paper.

Acknowledgements

This work did not receive any grant from the public, commercial, or not-for-profit funding agencies.

Appendix A. Supplementary material

Supplementary data to this article can be found online at https://doi.org/10.1016/j.matdes.2022.110511.

References

[1] I.M. El-Sherbiny, I.E. Elkholi, M.H. Yacoub, Tissue plasminogen activator-based clot busting: Controlled delivery approaches, Glob. Cardiol. Sci. Pract. (2014), https://doi.org/10.5339/gcsp.2014.46.
[2] S.E. Kimmel, J.A. Berlin, S. Hennessy, B.L. Strom, R.J. Krone, W.K. Laskey, Risk of major complications from coronary angioplasty performed immediately after diagnostic coronary angiography: Results from the registry of the society for cardiac angiography and interventions, J. Am. Coll. Cardiol. (1997), https://doi.org/10.1016/S0735-1097(97)00149-6.
[3] H. Schuhlen, A. Kastrati, J. Dirschinger, J. Hausleiter, S. Elezi, A. Wehinger, J. Pache, M. Hadamitzky, A. Schomig, Intracoronary stenting and risk for major adverse cardiac events during the first month, Circulation 98 (1998) 104–111.
[4] M.I. Tomey, A.S. Kini, S.K. Sharma, Current status of rotational atherectomy, JACC Cardiovasc Interv. 7 (2014) 345–353, https://doi.org/10.1016/j.jcin.2013.12.196.
[5] S. Jafarzadeh, A. Nasiri Sadr, E. Kaffash, S. Goudarzi, E. Golab, A. Karimipour, The Effect of Hematocrit and Nanoparticles Diameter on Hemodynamic Parameters and Drug Delivery in Abdominal Aortic Aneurysm with Consideration of Blood Pulsatile Flow, Comput. Methods Programs Biomed. (2020), https://doi.org/10.1016/j.cmpb.2020.105545.
[6] M. Satpathy, L. Wang, R.J. Zielinski, W. Qian, Y.A. Wang, A.M. Mohs, B.A. Kairdolf, X. Ji, J. Capala, M. Lipowska, S. Nie, H. Mao, L. Yang, Targeted drug delivery and image-guided therapy of heterogeneous ovarian cancer using HER2-targeted theranostic nanoparticles, Theranostics. (2019), https://doi.org/10.7150/thno.29964.
[7] P.Y. Liyanage, S.D. Hettiarachchi, Y. Zhou, A. Ouhtit, E.S. Seven, C.Y. Oztan, E. Celik, R.M. Leblanc, Nanoparticle-mediated targeted drug delivery for breast cancer treatment, Biochim. Biophys. Acta - Rev. Cancer. (2019), https://doi.org/10.1016/j.bbcan.2019.04.006.
[8] M.E. Peralta, S.A. Jadhav, G. Magnacca, D. Scalarone, D.O. Mártire, M.E. Parolo, L. Carlos, Synthesis and in vitro testing of thermoresponsive polymer-grafted core-shell magnetic mesoporous silica nanoparticles for efficient controlled and targeted drug delivery, J. Colloid Interface Sci. (2019), https://doi.org/10.1016/j.jcis.2019.02.086.
[9] T. Matoba, J. Ichiro Koga, K. Nakano, K. Egashira, H. Tsutsui, Nanoparticle-mediated drug delivery system for atherosclerotic cardiovascular disease, J. Cardiol. (2017), https://doi.org/10.1016/j.jjcc.2017.03.005.
[10] C. Fan, J. Joshi, F. Li, B. Xu, M. Khan, J. Yang, W. Zhu, Nanoparticle-Mediated Drug Delivery for Treatment of Ischemic Heart Disease, Front. Bioeng. Biotechnol. (2020), https://doi.org/10.3389/fbioe.2020.00687.
[11] M.E. DeBakey, G.M. Lawrie, D.H. Glaeser, Patterns of atherosclerosis and their surgical significance, Ann. of sur. 201 (2) (1985) 115.
[12] S. Muro, C. Garnacho, J.A. Champion, J. Leferovich, C. Gajewski, E.H. Schuchman, S. Mitragotri, V.R. Muzykantov, Control of endothelial targeting and intracellular delivery of therapeutic enzymes by modulating the size and shape of ICAM-1-targeted carriers, Mol. Ther. (2008), https://doi.org/10.1038/mt.2008.127.
[13] K. Namdee, A.J. Thompson, P. Charoenphol, O. Eniola-Adefeso, Margination propensity of vascular-targeted spheres from blood flow in a microfluidic model of human microvessels, Langmuir 29 (2013) 2530–2535, https://doi.org/10.1021/la304746p.
[14] A.J. Thompson, E.M. Mastria, O. Eniola-Adefeso, The margination propensity of ellipsoidal micro/nanoparticles to the endothelium in human blood flow, Biomaterials 34 (2013) 5863–5871, https://doi.org/10.1016/j.biomaterials.2013.04.011.
[15] K. Muller, D.A. Fedosov, G. Gompper, Margination of micro- and nano-particles in blood flow and its effect on drug delivery, Sci. Rep. 4 (2014) 4871, https://doi.org/10.1038/srep04871.
[16] K. Muller, D.A. Fedosov, G. Gompper, Understanding particle margination in blood flow - A step toward optimized drug delivery systems, Med. Eng. Phys. 38 (2016) 2–10, https://doi.org/10.1016/j.medengphy.2015.08.009.

[17] T.R. Lee, M. Choi, A.M. Kopacz, S.H. Yun, W.K. Liu, P. Decuzzi, On the near-wall accumulation of injectable particles in the microcirculation: Smaller is not better, Sci. Rep. (2013), https://doi.org/10.1038/srep02079.
[18] J.W. Nichols, Y. Sakurai, H. Harashima, Y.H. Bae, Nano-sized drug carriers: Extravasation, intratumoral distribution, and their modeling, J. Control. Release 267 (2017) 31–46, https://doi.org/10.1016/j.jconrel.2017.08.003.
[19] S.S. Hossain, Y. Zhang, X. Liang, F. Hussain, M. Ferrari, T.J. Hughes, P. Decuzzi, In silico vascular modeling for personalized nanoparticle delivery, Nanomedicine (Lond). 8 (2013) 343–357, https://doi.org/10.2217/nnm.12.124.
[20] S.S. Hossain, S.F.A. Hossainy, Y. Bazilevs, V.M. Calo, T.J.R. Hughes, Mathematical modeling of coupled drug and drug-encapsulated nanoparticle transport in patient-specific coronary artery walls, Comput. Mech. 49 (2011) 213–242, https://doi.org/10.1007/s00466-011-0633-2.
[21] F. Michor, J. Liphardt, M. Ferrari, J. Widom, What does physics have to do with cancer?, Nat Rev. Cancer 11 (2011) 657–670, https://doi.org/10.1038/nrc3092.
[22] M. Forouzandehmehr, J.T. Koivumäki, J. Hyttinen, M. Paci, A mathematical model of hiPSC cardiomyocytes electromechanics, Physiol. Rep. 9 (2021), https://doi.org/10.14814/phy2.15124.
[23] S. Sohrabi, J. Zheng, E.A. Finol, Y. Liu, Numerical simulation of particle transport and deposition in the pulmonary vasculature, J. Biomech. Eng. 136 (2014), https://doi.org/10.1115/1.4028800.
[24] S. Sohrabi, S. Wang, J. Tan, J. Xu, J. Yang, Y. Liu, Nanoparticle transport and delivery in a heterogeneous pulmonary vasculature, J. Biomech. 50 (2017) 240–247, https://doi.org/10.1016/j.jbiomech.2016.11.023.
[25] S.J. Zhu, E.K. Poon, A.S. Ooi, S. Moore, Enhanced targeted drug delivery through controlled release in a three-dimensional vascular tree, J. Biomech. Eng. 137 (2015), https://doi.org/10.1115/1.4028965.
[26] B. Godin, W.H. P. Driessen, B. Proneth, S.-Y. Lee, S. Srinivasan, R. Rumbaut, W. Arap, R. Pasqualini, M. Ferrari, P. Decuzzi, An Integrated Approach for the Rational Design of Nanovectors for Biomedical Imaging and Therapy, 69 (2010) 31–64. http://dx.doi.org/10.1016/s0065-2660(10)69009-8.
[27] J.W. Haverkort, S. Kenjereš, C.R. Kleijn, Computational Simulations of Magnetic Particle Capture in Arterial Flows, Ann. Biomed. Eng. 37 (2009) 2436–2448, https://doi.org/10.1007/s10439-009-9786-y.
[28] S. Kenjereš, B.W. Righolt, Simulations of magnetic capturing of drug carriers in the brain vascular system, Int. J. Heat Fluid Flow 35 (2012) 68–75, https://doi.org/10.1016/j.ijheatfluidflow.2012.03.008.
[29] A. Nacev, C. Beni, O. Bruno, B. Shapiro, The Behaviors of Ferro-Magnetic Nano-Particles In and Around Blood Vessels under Applied Magnetic Fields, J. Magn. Magn. Mater. 323 (2011) 651–668, https://doi.org/10.1016/j.jmmm.2010.09.008.
[30] T.S. Umbarkar, C. Kleinstreuer, Computationally Efficient Fluid-Particle Dynamics Simulations of Arterial Systems, Commun, Comput. Phys. 17 (2015) 401–423, https://doi.org/10.4208/cicp.160114.120914a.
[31] M. Epshtein, N. Korin, Computational and experimental investigation of particulate matter deposition in cerebral side aneurysms, J. R. Soc. Interface 17 (2020) 20200510, https://doi.org/10.1098/rsif.2020.0510.
[32] A. Shamloo, M. Forouzandehmehr, Personalised deposition maps for micro- and nanoparticles targeting an atherosclerotic plaque: attributions to the receptor-mediated adsorption on the inflamed endothelial cells, Biomech. Model. Mechanobiol. (2019), https://doi.org/10.1007/s10237-018-01116-y.
[33] Y. Asaad, M. Epshtein, A. Yee, N. Korin, The Flow Dependent Adhesion of von Willebrand Factor (VWF)-A1 Functionalized Nanoparticles in an in Vitro Coronary Stenosis Model, Molecules 24 (2019) 2679, https://doi.org/10.3390/molecules24152679.
[34] P. Eshtehardi, M.C. McDaniel, J. Suo, S.S. Dhawan, L.H. Timmins, J.N.G. Binongo, L.J. Golub, M.T. Corban, A.V. Finn, J.N. Oshinsk, A.A. Quyyumi, D.P. Giddens, H. Samady, Association of Coronary Wall Shear Stress With Atherosclerotic Plaque Burden, Composition, and Distribution in Patients With Coronary Artery Disease, J. Am. Heart Assoc. 1 (2012), https://doi.org/10.1161/JAHA.112.002543.
[35] M. Forouzandehmehr, A. Shamloo, High Haematocrit Blood Flow and Adsorption of Micro- and Nanoparticles on an Atherosclerotic Plaque: an in-silico study, Curr. Drug Deliv. 18 (2021), https://doi.org/10.2174/1567201818666210316111458.
[36] M. Forouzandehmehr, A. Shamloo, Margination and adhesion of micro- and nanoparticles in the coronary circulation: A step towards optimised drug carrier design, Biomech. Model. Mechanobiol. (2018), https://doi.org/10.1007/s10237-017-0955-x.
[37] B.M. Johnston, P.R. Johnston, S. Corney, D. Kilpatrick, Non-Newtonian blood flow in human right coronary arteries: steady state simulations, J. Biomech. 37 (2004) 709–720, https://doi.org/10.1016/j.jbiomech.2003.09.016.
[38] D.A. Fedosov, Multiscale Modeling of Blood Flow and Soft Matter, Brown University, 2010.
[39] S.Y. Lee, M. Ferrari, P. Decuzzi, Design of bio-mimetic particles with enhanced vascular interaction, J. Biomech. 42 (2009) 1885–1890, https://doi.org/10.1016/j.jbiomech.2009.05.012.
[40] W.E. Evans, H.L. McLeod, Pharmacogenomics–drug disposition, drug targets, and side effects, N. Engl. J. Med. 348 (2003) 538–549, https://doi.org/10.1056/NEJMra020526.
[41] R. Weinshilboum, Inheritance and drug response, N. Engl. J. Med. 348 (2003) 529–537, https://doi.org/10.1056/NEJMra020021.
[42] D.M. Kent, A. Alsheikh-Ali, R.A. Hayward, Competing risk and heterogeneity of treatment effect in clinical trials, Trials. 9 (2008) 30, https://doi.org/10.1186/1745-6215-9-30.
[43] D.M. Kent, R.A. Hayward, Limitations of applying summary results of clinical trials to individual patients: the need for risk stratification, JAMA 298 (2007) 1209–1212, https://doi.org/10.1001/jama.298.10.1209.
[44] S. Ghosh, Y. Matsuoka, Y. Asai, K.Y. Hsin, H. Kitano, Software for systems biology: from tools to integrated platforms, Nat. Rev. Genet. 12 (2011) 821–832, https://doi.org/10.1038/nrg3096.
[45] S. Nie, Nanotechnology for personalized and predictive medicine, Nanomedicine Nanotechnology, Biol. Med. 2 (2006), https://doi.org/10.1016/j.nano.2006.10.115.
[46] I.S. Vizirianakis, Handbook of Personalized Medicine: Advances in Nanotechnology, Drug Delivery, and Therapy, Pan Stanford, New York (2014), https://doi.org/10.4032/9789814411202.
[47] A. Amr, E. Kayvanpour, F. Sedaghat-Hamedani, T. Passerini, V. Mihalef, A. Lai, D. Neumann, B. Georgescu, S. Buss, D. Mereles, E. Zitron, A.E. Posch, M. Wurstle, T. Mansi, H.A. Katus, B. Meder, Personalized Computer Simulation of Diastolic Function in Heart Failure, Genomics Proteomics Bioinforma. 14 (2016) 244–252. http://dx.doi.org/10.1016/j.gpb.2016.04.006.
[48] L.M. Itu, P. Sharma, C. Suciu, Patient-specific Hemodynamic Computations: Application to Personalized Diagnosis of Cardiovascular Pathologies, 2017. http://dx.doi.org/10.1007/978-3-319-56853-9.
[49] E. Kayvanpour, T. Mansi, F. Sedaghat-Hamedani, A. Amr, D. Neumann, B. Georgescu, P. Seegerer, A. Kamen, J. Haas, K.S. Frese, M. Irawati, E. Wirsz, V. King, S. Buss, D. Mereles, E. Zitron, A. Keller, H.A. Katus, D. Comaniciu, B. Meder, Towards Personalized Cardiology: Multi-Scale Modeling of the Failing Heart, PLoS One 10 (2015) e0134869, https://doi.org/10.1371/journal.pone.0134869.
[50] S.S. Hossain, Y. Zhang, X. Fu, G. Brunner, J. Singh, T.J. Hughes, D. Shah, P. Decuzzi, Magnetic resonance imaging-based computational modelling of blood flow and nanomedicine deposition in patients with peripheral arterial disease, J. R. Soc. Interface 12 (2015), https://doi.org/10.1098/rsif.2015.0001.
[51] A.D. Caballero, S. Laín, Numerical simulation of non-Newtonian blood flow dynamics in human thoracic aorta, Comput. Methods Biomech. Biomed. Engin. 18 (2014) 1200–1216, https://doi.org/10.1080/10255842.2014.887698.
[52] [52] L. Goubergrits, E. Wellnhofer, U. Kertzscher, A. Katashev, Y. Dekhtyar, J. Spigulis, Choice and Impact of a Non-Newtonian Blood Model for Wall Shear Stress Profiling of Coronary Arteries, in: Springer Berlin Heidelberg, Berlin, Heidelberg, 2008: pp. 111–114.
[53] C. Oliveira, A.A. Soares, A. Simões, S. Gonzaga, A. Rouboa, Numerical Study of Non-Newtonian Blood Behavior in the Abdominal Aortic Bifurcation of a Patient-Specific at Rest, Open Sports Sci. J. 10 (2017) 279–285, https://doi.org/10.2174/1875399x01710010279.
[54] M. Sarmadi, A.M. Behrens, K.J. McHugh, H.T.M. Contreras, Z.L. Tochka, X. Lu, R. Langer, A. Jaklenec, Modeling, design, and machine learning-based framework for optimal injectability of microparticle-based drug formulations, Sci. Adv. 6 (2020) eabb6594, https://doi.org/10.1126/sciadv.abb6594.
[55] R. Picetti, H. Shakur-Still, R.L. Medcalf, J.F. Standing, I. Roberts, What concentration of tranexamic acid is needed to inhibit fibrinolysis? A systematic review of pharmacodynamics studies, Blood Coagul. Fibrinolysis 30 (2019) 1–10, https://doi.org/10.1097/MBC.0000000000000789.
[56] B.E. Bannish, I.N. Chernysh, J.P. Keener, A.L. Fogelson, J.W. Weisel, Molecular and Physical Mechanisms of Fibrinolysis and Thrombolysis from Mathematical Modeling and Experiments, Sci. Rep. 7 (2017) 6914, https://doi.org/10.1038/s41598-017-06383-w.
[57] S. Shah, Numerical Simulation of Particle Adhesion Dynamics For Applications In Nanomedicine And Biosensing, University of Texas at Arlington, 2009.
[58] A.A. Abba, B.A. Wani, R.A. Rahmatullah, M.Z. Khalil, A.M. Kumo, M.A. Ghonaim, Door to needle time in administering thrombolytic therapy for acute myocardial infarction, Saudi Med. J. 24 (2003) 361–364.
[59] M.R. Ali, M. Salim Hossain, M.A. Islam, M. Saiful Islam Arman, G. Sarwar Raju, P. Dasgupta, T.F. Noshin, Aspect of thrombolytic therapy: a review, ScientificWorldJournal. 2014 (2014) 586510. http://dx.doi.org/10.1155/2014/586510.
[60] F.W. Verheugt, B.J. Gersh, P.W. Armstrong, Aborted myocardial infarction: a new target for reperfusion therapy, Eur Hear. J. 27 (2006) 901–904, https://doi.org/10.1093/eurheartj/ehi829.
[61] [61] N. Korin, M. Kanapathipillai, B.D. Matthews, M. Crescente, A. Brill, T. Mammoto, K. Ghosh, S. Jurek, S.A. Bencherif, D. Bhatta, A.U. Coskun, C.L. Feldman, D.D. Wagner, D.E. Ingber, Shear-activated nanotherapeutics for drug targeting to obstructed blood vessels, Science (80-.). 337 (2012) 738–742. http://dx.doi.org/10.1126/science.1217815.
[62] A. Amani, A. Shamloo, S. Barzegar, M. Forouzandehmehr, Effect of Material and Population on the Delivery of Nanoparticles to an Atherosclerotic Plaque: A Patient-specific In Silico Study, Langmuir (2021), https://doi.org/10.1021/acs.langmuir.0c03158.
[63] I.D. Madukauwa-David, V. Sadri, P.A. Midha, V. Babaliaros, C. Aidun, A.P. Yoganathan, An Evaluation of the Influence of Coronary Flow on Transcatheter Heart Valve Neo-Sinus Flow Stasis, Ann. Biomed. Eng. 48 (2020) 169–180, https://doi.org/10.1007/s10439-019-02324-y.

[64] P. Decuzzi, R. Pasqualini, W. Arap, M. Ferrari, Intravascular delivery of particulate systems: does geometry really matter?, Pharm Res. 26 (2009) 235–243, https://doi.org/10.1007/s11095-008-9697-x.
[65] R.E. Serda, Mass Transport of Nanocarriers, Pan Stanford, 2012. https://books.google.com/books?id=O92kFjjfNzUC.
[66] U. Bagge, R. Karlsson, Maintenance of white blood cell margination at the passage through small venular junctions, Microvascular research. 20 (1) (1980) 92–95.
[67] H.L. Goldsmith, S. Spain, Margination of leukocytes in blood flow through small tubes, Microvascular research. 27 (2) (1984) 204–222.
[68] B. Woldhuis, G.J. Tangelder, D.W. Slaaf, R.S. Reneman, Concentration profile of blood platelets differs in arterioles and venules, Am. J. Physiol. 262 (1992) 1217–1223.
[69] G.J. Tangelder, H.C. Teirlinck, D.W. Slaaf, R.S. Reneman, Distribution of blood platelets flowing in arterioles, Am. J. of Physiol-Heart and Circ. Phys. 248 (3) (1985) 318–323.
[70] E.C. Eckstein, A.W. Tilles, F.J. Millero 3rd, Conditions for the occurrence of large near-wall excesses of small particles during blood flow, Microvasc. Res. 36 (1988) 31–39.
[71] A.W. Tilles, E.C. Eckstein, The near-wall excess of platelet-sized particles in blood flow: its dependence on hematocrit and wall shear rate, Microvasc. Res. 33 (1987) 211–223.
[72] J.D. Slack, M. Kanke, G.H. Simmons, P.P. DeLuca, Acute hemodynamic effects and blood pool kinetics of polystyrene microspheres following intravenous administration, J. Pharm. Sci. 70 (1981) 660–664.
[73] F. Gentile, C. Chiappini, D. Fine, R.C. Bhavane, M.S. Peluccio, M.M. Cheng, X. Liu, M. Ferrari, P. Decuzzi, The effect of shape on the margination dynamics of non-neutrally buoyant particles in two-dimensional shear flows, J. Biomech. 41 (2008) 2312–2318, https://doi.org/10.1016/j.jbiomech.2008.03.021.
[74] S. Dasgupta, T. Auth, G. Gompper, Wrapping of ellipsoidal nano-particles by fluid membranes, Soft Matter. 9 (22) (2013) 5473–5482.
[75] P. Decuzzi, M. Ferrari, The adhesive strength of non-spherical particles mediated by specific interactions, Biomaterials 27 (2006) 5307–5314, https://doi.org/10.1016/j.biomaterials.2006.05.024.
[76] K. Namdee, A.J. Thompson, A. Golinski, S. Mocherla, D. Bouis, O. Eniola-Adefeso, In vivo evaluation of vascular-targeted spheroidal microparticles for imaging and drug delivery application in atherosclerosis, Atherosclerosis. 237 (2014) 279–286, https://doi.org/10.1016/j.atherosclerosis.2014.09.025.
[77] S. Glagov, E. Weisenberg, C.K. Zarins, R. Stankunavicius, G.J. Kolettis, Compensatory enlargement of human atherosclerotic coronary arteries, New England Journal of Medicine. 316 (22) (1987) 1371–1375.
[78] T.M. Maul, D.D. Dudgeon, M.T. Beste, D.A. Hammer, J.S. Lazo, F.S. Villanueva, W.R. Wagner, Optimization of ultrasound contrast agents with computational models to improve selection of ligands and binding strength, Biotechnol. Bioeng. 107 (2010) 854–864, https://doi.org/10.1002/bit.22857.
[79] F.S. Villanueva, E. Lu, S. Bowry, S. Kilic, E. Tom, J. Wang, J. Gretton, J.J. Pacella, W.R. Wagner, Myocardial ischemic memory imaging with molecular echocardiography, Circulation 115 (2007) 345–352, https://doi.org/10.1161/CIRCULATIONAHA.106.633917.
[80] B.A. Kaufmann, J.M. Sanders, C. Davis, A. Xie, P. Aldred, I.J. Sarembock, J.R. Lindner, Molecular imaging of inflammation in atherosclerosis with targeted ultrasound detection of vascular cell adhesion molecule-1, Circulation 116 (2007) 276–284, https://doi.org/10.1161/CIRCULATIONAHA.106.684738.
[81] K. Khodabandehlou, J.J. Masehi-Lano, C. Poon, J. Wang, E.J. Chung, Targeting cell adhesion molecules with nanoparticles using in vivo and flow-based in vitro models of atherosclerosis, Exp. Biol. Med. 242 (2017) 799–812, https://doi.org/10.1177/1535370217693116.
[82] V.R. Muzykantov, Targeted Drug Delivery to Endothelial Adhesion Molecules, ISRN Vasc. Med. 2013 (2013) 1–27, https://doi.org/10.1155/2013/916254.
[83] G.E. Weller, E. Lu, M.M. Csikari, A.L. Klibanov, D. Fischer, W.R. Wagner, F.S. Villanueva, Ultrasound imaging of acute cardiac transplant rejection with microbubbles targeted to intercellular adhesion molecule-1, Circulation 108 (2003) 218–224, https://doi.org/10.1161/01.CIR.0000080287.74762.60.
[84] K. Jin, Z. Luo, B. Zhang, Z. Pang, Biomimetic nanoparticles for inflammation targeting, Acta Pharm Sin B. 8 (2018) 23–33, https://doi.org/10.1016/j.apsb.2017.12.002.
[85] P.K. Shah, Role of inflammation and metalloproteinases in plaque disruption and thrombosis, Vasc. Med. 3 (2016) 199–206, https://doi.org/10.1177/1358836x9800300304.
[86] C. Sun, J.S. Lee, M. Zhang, Magnetic nanoparticles in MR imaging and drug delivery, Adv. Drug Deliv. Rev. 60 (2008) 1252–1265, https://doi.org/10.1016/j.addr.2008.03.018.
[87] R. Krzyminiewski, B. Dobosz, G. Schroeder, J. Kurczewska, Focusing of Fe3O4 nanoparticles using a rotating magnetic field in various environments, Phys. Lett. Sect. A Gen. At. Solid State Phys. (2018), https://doi.org/10.1016/j.physleta.2018.07.051.
[88] A. Nacev, I.N. Weinberg, P.Y. Stepanov, S. Kupfer, L.O. Mair, M.G. Urdaneta, M. Shimoji, S.T. Fricke, B. Shapiro, Dynamic inversion enables external magnets to concentrate ferromagnetic rods to a central target, Nano Lett. (2015), https://doi.org/10.1021/nl503654t.
[89] A. Patronis, R.A. Richardson, S. Schmieschek, B.J.N. Wylie, R.W. Nash, P.V. Coveney, Modeling patient-specific magnetic drug targeting within the intracranial vasculature, Front. Physiol. (2018), https://doi.org/10.3389/fphys.2018.00331.
[90] S. Kenjereš, Modeling and simulation of multi-physics multi-scale transport phenomenain bio-medical applications, J. Phys. Conf. Ser. (2014), https://doi.org/10.1088/1742-6596/530/1/012006.
[91] T. Neuberger, B. Schöpf, H. Hofmann, M. Hofmann, B. Von Rechenberg, Superparamagnetic nanoparticles for biomedical applications: Possibilities and limitations of a new drug delivery system, J. Magn. Magn. Mater. 293 (2005) 483–496, https://doi.org/10.1016/j.jmmm.2005.01.064.
[92] O. Veiseh, C. Sun, J. Gunn, N. Kohler, P. Gabikian, D. Lee, N. Bhattarai, R. Ellenbogen, R. Sze, A. Hallahan, J. Olson, M. Zhang, Optical and MRI multifunctional nanoprobe for targeting gliomas, Nano Lett. 5 (2005) 1003–1008, https://doi.org/10.1021/nl0502569.
[93] Y. Zhang, N. Kohler, M. Zhang, Surface modification of superparamagnetic magnetite nanoparticles and their intracellular uptake, Biomaterials 23 (2002) 1553–1561, https://doi.org/10.1016/s0142-9612(01)00267-8.
[94] A.S. Lubbe, C. Alexiou, C. Bergemann, Clinical applications of magnetic drug targeting, J. Surg. Res. 95 (2001) 200–206, https://doi.org/10.1006/jsre.2000.6030.
[95] M. Momeni Larimi, A. Ramiar, A.A. Ranjbar, Magnetic nanoparticles and blood flow behavior in non-Newtonian pulsating flow within the carotid artery in drug delivery application, Proc. Inst. Mech. Eng. Part H J. Eng. Med. (2016), https://doi.org/10.1177/0954411916656663.
[96] M.M. Larimi, A. Ramiar, A.A. Ranjbar, Numerical simulation of magnetic nanoparticles targeting in a bifurcation vessel, J. Magn. Magn. Mater. (2014), https://doi.org/10.1016/j.jmmm.2014.03.002.
[97] M.D. Tehrani, J.H. Yoon, M.O. Kim, J. Yoon, A novel scheme for nanoparticle steering in blood vessels using a functionalized magnetic field, IEEE Trans. Biomed. Eng. (2015), https://doi.org/10.1109/TBME.2014.2351234.
[98] A. Krafcik, P. Babinec, I. Frollo, Computational analysis of magnetic field induced deposition of magnetic particles in lung alveolus in comparison to deposition produced with viscous drag and gravitational force, J. Magn. Magn. Mater. (2014), https://doi.org/10.1016/j.jmmm.2014.10.018.
[99] M.M. Larimi, A. Ramiar, A.A. Ranjbar, Numerical simulation of magnetic drug targeting with Eulerian-Lagrangian model and effect of viscosity modification due to diabetics, Appl. Math. Mech. English Ed. (2016). http://dx.doi.org/10.1007/s10483-016-2145-8.
[100] A. Boghi, F. Russo, F. Gori, Numerical simulation of magnetic nano drug targeting in a patient-specific coeliac trunk, J. Magn. Magn. Mater. (2017), https://doi.org/10.1016/j.jmmm.2017.04.055.
[101] S. Kenjereš, J.L. Tjin, Numerical simulations of targeted delivery of magnetic drug aerosols in the human upper and central respiratory system: A validation study, R. Soc. Open Sci. (2017), https://doi.org/10.1098/rsos.170873.
[102] S.L. Raut, B. Kirthivasan, M.M. Bommana, E. Squillante, M. Sadoqi, The formulation, characterization and in vivo evaluation of a magnetic carrier for brain delivery of NIR dye, Nanotechnology. (2010), https://doi.org/10.1088/0957-4484/21/39/395102.
[103] S. Wang, X. Guo, L. Ren, B. Wang, L. Hou, H. Zhou, Q. Gao, Y. Gao, L. Wang, Targeting and deep-penetrating delivery strategy for stented coronary artery by magnetic guidance and ultrasound stimulation, Ultrason. Sonochem. 67 (2020), https://doi.org/10.1016/j.ultsonch.2020.105188.
[104] A. Shamloo, A. Amani, M. Forouzandehmehr, I. Ghoytasi, In silico study of patient-specific magnetic drug targeting for a coronary LAD atherosclerotic plaque, Int. J. Pharm. (2019), https://doi.org/10.1016/j.ijpharm.2018.12.088.
[105] G.I. Bell, M. Dembo, P. Bongrand, Cell adhesion. Competition between nonspecific repulsion and specific bonding, Biophys. J. 45 (1984) 1051–1064, https://doi.org/10.1016/s0006-3495(84)84252-6.
[106] D.A. Hammer, D.A. Lauffenburger, A dynamical model for receptor-mediated cell adhesion to surfaces, Biophys. J. 52 (1987) 475–487, https://doi.org/10.1016/s0006-3495(87)83236-8.
[107] K.-C. Chang, D.A. Hammer, Adhesive Dynamics Simulations of Sialyl-Lewisx/E-selectin-Mediated Rolling in a Cell-Free System, Biophys. J. 79 (2000) 1891–1902, https://doi.org/10.1016/s0006-3495(00)76439-3.
[108] E.F. Krasik, K.E. Caputo, D.A. Hammer, Adhesive dynamics simulation of neutrophil arrest with stochastic activation, Biophys. J. (2008), https://doi.org/10.1529/biophysj.107.119677.
[109] A.J. Goldman, R.G. Cox, H. Brenner, Slow viscous motion of a sphere parallel to a plane wall—II Couette flow, Chem. Eng. Sci. 22 (1967) 653–660, https://doi.org/10.1016/0009-2509(67)80048-4.
[110] A.M. Wierenga, T.A.J. Lenstra, A.P. Philipse, Aqueous dispersions of colloidal gibbsite platelets: Synthesis, characterisation and intrinsic viscosity measurements, Colloids Surfaces A Physicochem. Eng. Asp. (1998), https://doi.org/10.1016/S0927-7757(97)00224-0.
[111] A. Illing, T. Unruh, M.H.J. Koch, Investigation on particle self-assembly in solid lipid-based colloidal drug carrier systems, Pharm. Res. (2004), https://doi.org/10.1023/B:PHAM.0000022405.49805.a7.
[112] J.P. Rolland, B.W. Maynor, L.E. Euliss, A.E. Exner, G.M. Denison, J.M. DeSimone, Direct fabrication and harvesting of monodisperse, shape-specific nanobiomaterials, J. Am. Chem. Soc. (2005), https://doi.org/10.1021/ja051977c.
[113] A.B. Subramaniam, M. Abkarian, L. Mahadevan, H.A. Stone, Colloid science: Non-spherical bubbles, Nature (2005), https://doi.org/10.1038/438930a.
[114] X. Chen, R. Wong, I. Khalidov, A.Y. Wang, J. Leelawattanachai, Y. Wang, M.M. Jin, Inflamed leukocyte-mimetic nanoparticles for molecular imaging of inflammation, Biomaterials 32 (2011) 7651–7661, https://doi.org/10.1016/j.biomaterials.2011.06.030.

[115] G.E. Weller, F.S. Villanueva, A.L. Klibanov, W.R. Wagner, Modulating targeted adhesion of an ultrasound contrast agent to dysfunctional endothelium, Ann. Biomed. Eng. 30 (2002) 1012–1019, https://doi.org/10.1114/1.1513565.
[116] M. Long, H. Zhao, K.-S. Huang, C. Zhu, Kinetic Measurements of Cell Surface E-Selectin/Carbohydrate Ligand Interactions, Ann. Biomed. Eng. 29 (2001) 935–946, https://doi.org/10.1114/1.1415529.
[117] B.J. Kirby, Micro- and Nanoscale Fluid Mechanics: Transport in Microfluidic Devices, Cambridge University Press, 2010. https://books.google.co.uk/books?id=y7PB9f5zmU4C.
[118] R. Turton, O. Levenspiel, A short note on the drag correlation for spheres, Powder Technol. (1986), https://doi.org/10.1016/0032-5910(86)80012-2.
[119] P.G. Saffman, The lift on a small sphere in a slow shear flow, J. Fluid Mech. 22 (1965) 385–400, https://doi.org/10.1017/S0022112065000824.
[120] N.A. Mody, M.R. King, Influence of Brownian motion on blood platelet flow behavior and adhesive dynamics near a planar wall, Langmuir 23 (2007) 6321–6328, https://doi.org/10.1021/la0701475.
[121] R.L. Fournier, Basic Transport Phenomena in Biomedical Engineering, third ed., Taylor & Francis, 2011. https://books.google.com/books?id=BcXUOFjoZPMC.
[122] A.D. Grief, G. Richardson, Mathematical modelling of magnetically targeted drug delivery, J. Magn. Magn. Mater. 293 (2005) 455–463, https://doi.org/10.1016/j.jmmm.2005.02.040.
[123] M. Kim, Effect of electrostatic, hydrodynamic, and Brownian forces on particle trajectories and sieving in normal flow filtration, J. Colloid Interface Sci. 269 (2004) 425–431, https://doi.org/10.1016/j.jcis.2003.08.004.
[124] A. Li, G. Ahmadi, Dispersion and Deposition of Spherical Particles from Point Sources in a Turbulent Channel Flow, Aerosol Sci. Technol. 16 (1992) 209–226, https://doi.org/10.1080/02786829208959550.
[125] E.P. Furlani, Magnetophoretic separation of blood cells at the microscale, J. Phys. D Appl. Phys. (2007), https://doi.org/10.1088/0022-3727/40/5/001.
[126] Myung Ki Baek, Hong Soon Choi, Ki Sik Lee, Il Han Park, Numerical Analysis for Magnetophoretic Separation of Blood Cells in Fluid and Magnetic Field, IEEE Trans. Appl. Supercond. 22 (2012) 4401604–4401604. http://dx.doi.org/10.1109/TASC.2011.2174584.
[127] J.F. Schenck, The role of magnetic susceptibility in magnetic resonance imaging: MRI magnetic compatibility of the first and second kinds, Med. Phys. 23 (1996) 815–850, https://doi.org/10.1118/1.597854.
[128] [128] MUMPS: MUltifrontal Massively Parallel sparse direct Solver, (n.d.). http://mumps.enseeiht.fr/.
[129] U.M.. P. Ascher L. R., Computer Methods for Ordinary Differential Equations and Differential-Algebraic Equations, SIAM, Philadelphia, 1998.
[130] C.F. Curtiss, J.O. Hirschfelder, Integration of Stiff Equations, Proc. Natl. Acad. Sci. U. S. A. 38 (1952) 235–243.
[131] J. Chung, G.M. Hulbert, A time integration algorithm for structural dynamics with improved numerical dissipation: The generalized-α method, J. Appl. Mech. Trans. ASME. (1993), https://doi.org/10.1115/1.2900803.
[132] K.E. Jansen, C.H. Whiting, G.M. Hulbert, Generalized-α method for integrating the filtered Navier-Stokes equations with a stabilized finite element method, Comput. Methods Appl. Mech. Eng. (2000), https://doi.org/10.1016/S0045-7825(00)00203-6.
[133] A. Shamloo, M.A. Nejad, M. Saeedi, Fluid–structure interaction simulation of a cerebral aneurysm: Effects of endovascular coiling treatment and aneurysm wall thickening, J. Mech. Behav. Biomed. Mater. (2017), https://doi.org/10.1016/j.jmbbm.2017.05.020.
[134] A. Shamloo, M.Z. Pedram, H. Heidari, A. Alasty, Computing the blood brain barrier (BBB) diffusion coefficient: A molecular dynamics approach, J. Magn. Magn. Mater. (2017), https://doi.org/10.1016/j.jmmm.2016.03.030.
[135] A. Shamloo, N. Mohammadaliha, M. Mohseni, Integrative Utilization of Microenvironments, Biomaterials and Computational Techniques for Advanced Tissue Engineering, J. Biotechnol. (2015).
[136] A. Shamloo, S. Ebrahimi, A. Amani, F. Fallah, Targeted Drug Delivery of Microbubble to Arrest Abdominal Aortic Aneurysm Development: A Simulation Study Towards Optimized Microbubble Design, Sci. Rep. (2020), https://doi.org/10.1038/s41598-020-62410-3.